Formation of Fibrous Materials from Dense Calcium Caseinate Dispersions

Julita M. Manski, Atze J. van der Goot,* and Remko M. Boom

Food and Bioprocess Engineering Group, Wageningen University, P.O. Box 8129, 6700 EV Wageningen, The Netherlands

Received October 19, 2006; Revised Manuscript Received December 19, 2006

Application of shear and cross-linking enzyme transglutaminase (Tgase) induced fibrous hierarchical structures in dense (30% w/w) calcium caseinate (Ca-caseinate) dispersions. Using Tgase was essential for the anisotropic structure formation. The fibrous materials showed anisotropy on both micro- and macroscale as determined with scanning electron microscopy (SEM) and mechanical analyses, respectively. SEM revealed protein fibers with a diameter of ∼100−200 nm; visually, we observed fibers of about 1 mm. Both shear and Tgase affected the reinforcement of the fibers to a large extent, whereas the mechanical properties in the direction perpendicular to the shear flow remained constant. Shearing Ca-caseinate without Tgase yielded a slightly anisotropic layered structure. Both cross-linking in the absence of shear and cross-linking during mixing resulted in gels without alignment. The formation of shear- and enzyme-induced anisotropic structures was explained by aligning of protein aggregates due to shear and concurrent solidification of the aligned protein aggregates.

Introduction

The formation of fibrous food textures has received much interest from industry as well as food scientists for several decades. Replacing meat products with products from alternative protein sources is an important challenge. This implies creating meat-like structural and sensory properties with non-meat protein-based materials, that is, the formation of anisotropic structures at various length scales and in various concentration regimes.[1,2] Research on fibrous protein materials can be divided roughly into the self-assembly of proteins into fibrils, and the forced assembly of proteins into fibrous textures. Fibrillar self-assembly of various proteins, such as β-lactoglobulin, ovalbumin, and bovine serum albumin, has been achieved in diluted and semidiluted regimes under severe pH and temperature conditions.[3,4] These fibrils were in the order of nanometers thick and micrometers long. In contrast to self-assembly, forced assembly of protein solutions in the concentrated regime (e.g., >10% w/w protein) has been approached traditionally using extrusion or spinning techniques.

Extrusion cooking has been used to texturize proteins from various sources, such as soy flours, wheat, and dairy proteins.[2,5] Plasticization, melting, and break-up of proteins occur in the extruder barrel, and fibrous textures can be formed due to alignment of the proteins in long cooling dies.[2,5] Cheftel obtained fibrous structures only from soy concentrate; soy isolates could not be transformed into anisotropic structures.[5] Typical values of ratio of the longitudinal and transverse resistance to stretching are 1−4 for fibrous extrudates from defatted soy flour, depending on the barrel temperature and pH.[6] This ratio, indicative of fiber quality,[7] was 1−2 for extrudates of defatted soy flour and pork as determined by cutting.[8] Tolstoguzov underlined that incompatible biopolymers are required to form anisotropic structures during extrusion.[9] In general, the shortcomings of extrusion are the use of high temperatures for protein denaturation, inducing uncontrollable chemical reactions, and the presence of high shear forces during extrusion, which can lead to break-up of structural elements,[10] even at a molecular level.[11]

Spinning of biopolymers is based on aligning macromolecules due to shear and elongational flow in a spinneret and during coagulation.[12] Typically, the resulting fibers (∼100 μm) are coagulated in baths containing acid and salt solutions, and then washed. Hydrocolloids, such as carrageenan[13,14] and alginate,[15,16] or vegetable proteins, such as soy[17] or field bean protein,[18] were used in combination with casein in a two-phase blend to decrease the solubility in water of the casein-based fibers produced. In the case of spun pea and fababean protein, fibers with a granular core and strand-like cortex were formed.[12] Edible films prepared using wet spinning of soy protein isolate did not reveal any macromolecular orientation of the proteins.[19] The disadvantages of spinning are the large waste streams of water from the coagulation and washing baths. In addition, the necessity for low pH, high salt concentrations, and chemical additives to coagulate the fibers makes the design of a process for production of fibers suitable for consumption a complex matter.

In this paper, we present a novel technology based on application of simple shear flow and concurrent enzymatic cross-linking to induce an anisotropic fibrous structure in concentrated calcium caseinate without the necessity for coagulation baths, washing steps, high temperatures, or high shear forces.

Casein consists mainly of α_{S1}-, α_{S2}-, β-, and κ-casein in the ratio 4:4:2:1. The serine and threonyl phosphates of α- and β-caseins can interact with calcium (Ca^{2+}) and other di- and trivalent ions.[20] Because of this interaction, calcium caseinate (Ca-caseinate) dispersions contain protein aggregates[21,22] that are comparable with casein micelles (∼100−300 nm) in milk.[23,24] Sodium caseinate, dialyzed with ionic Ca^{2+} at various concentrations, featured a hydrodynamic radius in the range of ∼100−300 nm, which indicates the presence of aggregates of at least hundreds of protein molecules.[24] The enzyme transglutaminase (Tgase) has been used mainly to cross-link sodium caseinate.[25−27] We examined the susceptibility of Ca-caseinate to alignment by shear and solidification by Tgase, because Ca-

* Corresponding author. Phone: +31 317 484372. Fax: +31 317 482237. E-mail: atzejan.vandergoot@wur.nl.

10.1021/bm061008p CCC: $37.00 © 2007 American Chemical Society
Published on Web 02/28/2007

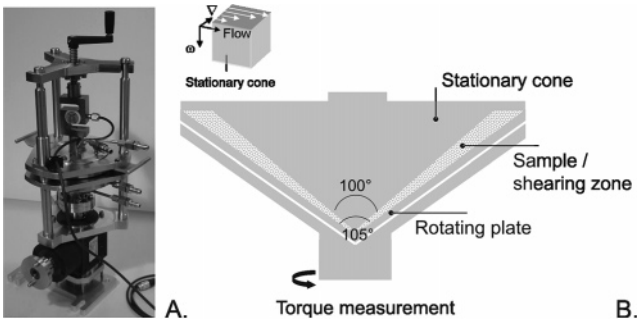

Figure 1. Picture (A) and schematic overview (B) of the shear cell device. The cone angle = 100°; the angle between the cone and the plate (shearing zone) = 2.5°; R_{plate} = 0.08508 m; R_{cone} = 0.07638 m. The stationary cone and rotating plate are heated/cooled with water.

caseinate dispersions comprise larger protein aggregates than sodium caseinate (~50 nm).[28] To our knowledge, the enzymatic gelation of Ca-caseinate has not been studied before.

In this paper, we show that simple shear and enzymatic cross-linking induces a novel fibrous protein structure based on Ca-caseinate only. The resulting microstructural properties were studied with SEM analysis. The structural characteristics are revealed with small and large deformations leading to the linear viscoelastic properties and the mechanical properties, respectively, of the Ca-caseinate structures.

Experimental Section

Materials. The measured activity of microbial Ca^{2+}-independent transglutaminase (protein-glutamine:amine γ-glutamyl-transferase, EC 2.3.2.13) derived from *Streptoverticilium moberansae* (1% Tgase, 99% maltodextrine, Ajinomoto Co. Inc., Tokyo, Japan) was 117 units g^{-1} using the hydroxamate method.[29] Tgase catalyzes acyl-transfer reactions between γ-carboxyamide groups of glutamine and the ϵ-amino group of lysines in proteins. A 20% (w/w in demineralized water) Tgase solution was freshly prepared prior to the experimental runs by mechanical stirring at room temperature for 1 h.

Ca-caseinate contained at least 88% protein according to the manufacturer's specifications (DMV International, Veghel, The Netherlands). A protein premix (pH 6.8−7.0) consisting of 30% w/w Ca-caseinate, Tgase (enzyme/protein (E:P) ratio 1:20 based on weight), and demineralized water was prepared in a kitchen mixer at low speed and at room temperature prior to processing. Some minor components were added for preservation and further analysis (confocal laser scanning microscopy: data not shown), such as 1% (w/w) sodium benzoate (Sigma Aldrich, Zwijndrecht, The Netherlands) and 2×10^{-4}% (w/w) Rhodamine 110 (83695, Sigma Aldrich), added as a 0.02 g L^{-1} solution in phosphate buffered saline (PBS).

Dimethylsulfoxide (DMSO) and ethanol used for the preparation of samples for SEM were of analytical grade (Sigma Aldrich).

Shear Cell Device. A well-defined flow was applied by using the shear cell device developed in house (Wageningen University, The Netherlands), based on a rheometer concept[30] and depicted in Figure 1A. In the shear cell device (V = 70 mL), biopolymers are subjected to a simple linear shear profile, which is established between the plate (i.e., the bottom cone) and the cone (angle α_{plate} = 105°, α_{cone} = 100°) as shown in the schematic drawing (Figure 1B). The rotating plate and stationary cone are heated (or cooled) with water. The temperature of the material is measured with a thermo couple located in the cone. The device is attached to a Brabender Do-Corder 330 (Brabender OHG, Duisburg, Germany) to enable shear rate control, and torque and temperature readings.

Sample Preparation in the Shear Cell Device. The Ca-caseinate premix prepared in the kitchen mixer was transferred to the pre-heated (50 °C) shear cell device. After the shear cell was filled, the mixture was subjected to the following shear treatment: 4 min at 5 rpm (12 s^{-1}), then an increase from 5 to 50 rpm (12 to 120 s^{-1}) within 1 min, and then 30 min at 50 rpm (120 s^{-1}). In the case of a quiescent treatment, the mixture was subjected to 5 rpm for 30 s, and subsequently the shear cell was stopped (0 rpm) for 35 min. In addition, a Ca-caseinate sample was prepared in a mixing bowl (W-50, Brabender OHG) with counter rotating elements, which was attached to the Brabender Do-Corder, at the same rotational speed as the sheared samples prepared in the shear cell device. After processing, the material was cooled in the stationary shear cell to approximately 12 °C in ~10 min. The mixed material was not cooled, but a sample was taken immediately at 50 °C. The processed materials were transferred to moulds consisting of two square parallel plates. Part of the material was used within 2 h for further analysis (tensile tests and sample preparation for SEM), and some was stored in a refrigerator for 1 day at 4 °C until further analysis (protein content and linear viscoelastic (LVE) measurements). The time between creating the materials and performing specific measurements was kept constant.

Scanning Electron Microscopy. Micro- and nanostructural aspects of the Ca-caseinate materials were observed with a field emission scanning electron microscope (FESEM) at ambient temperature. Dry samples were prepared according to the modified method described by Muller et al.[31] to observe the protein network without interference of the water phase. Sheared Ca-caseinate samples were carefully cut into squares (<10 × 10 mm) and immersed in DMSO (concentration range 15%, 30%, and 50% v/v in demineralized water) for 60 min each. Excess 50% DMSO was removed from the samples with filter paper. Slow freezing of the samples was performed in cold gaseous nitrogen above liquid nitrogen. Subsequently, the samples were immersed in liquid nitrogen, and freeze fractured on a brass table with a razorblade (single edge carbon steel, EMS, WA) and a hammer. Freeze fracturing was performed parallel and perpendicular to the shear flow that was exerted on the samples in the shear cell device (based on the shear flow−vorticity plane). The resulting fracture planes were the velocity gradient−shear flow plane and velocity gradient−vorticity plane, respectively. In this paper, we define the directions and resulting fracture planes as parallel and perpendicular, respectively. The mixed sample, having no clear shear direction, was treated similarly after defining a random plane (plane 1), and a plane perpendicular to this plane (plane 2). All of the Ca-caseinate samples exhibited brittle fracture. After fracturing, samples were thawed in 50% DMSO for >60 min, and subsequently rehydrated with water through the reverse DMSO concentration range (60 min each). The samples were dehydrated in graded series of ethanol (10%, 30%, 50%, 70%, 90% v/v) to 100% ethanol (20 min each). Samples in 100% ethanol were critical point dried with carbon dioxide (CPD 020, Balzers, Liechtenstein) and examined with a stereomicroscope to identify the fracture planes. Subsequently, the samples were glued on a sample holder using conductive carbon cement (Leit-C, Neubauer Chemicalien, Germany), and sputter coated with 20 nm platinum (JFC 1200, JEOL, Japan). The fractured surfaces were analyzed with a FESEM (JEOL 6300 F, Tokyo, Japan) at room temperature at a working distance of 8 mm, with SE detection at 3.5−5 kV. All images were recorded digitally (Orion, 6 E.L.I. sprl., Belgium) at a scan rate of 100 s (full frame) at a size of 2528 × 2030, 8 bit. Noise reduction and resizing of the images were done using Adobe Photoshop CS.

Rheological Properties. The LVE properties (G' and tan δ) were determined in duplicate with dynamic oscillating strain amplitude tests with a stress-controlled Bohlin CVO (Bohlin Instruments Ltd., Cirencester, UK) at a constant frequency of 1 Hz and at a temperature of 20 °C. Serrated parallel plates (diameter 25 mm, gap 2 mm) were used to prevent slipping. A chamber covering the sample was used to prevent evaporation. Before measuring, the samples were rested for 15 min to allow relaxation of the stresses induced by sample loading.

Mechanical Properties. A Texture Analyzer T2 (Stable Micro Systems Ltd., Surrey, UK) was used for large deformation tests. Uni-

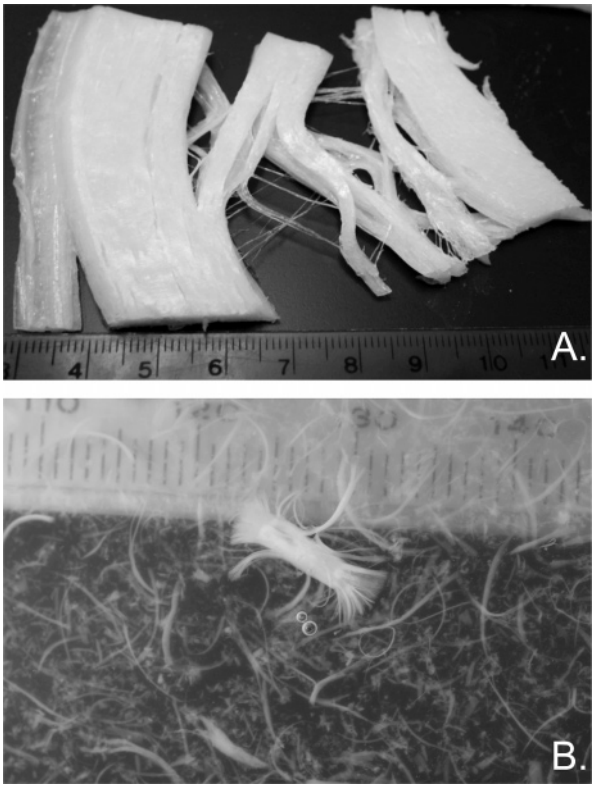

Figure 2. Picture of fibrous 30% Ca-caseinate after shearing and cross-linking (A). After a piece of the same sample was suspended in demi-water for 1 day, distinct fibers were visible (B). The scale in both pictures is in centimeters.

axial tensile tests were conducted with a constant deformation rate of 3 mm s^{-1} at room temperature within 2 h after creating the Ca-caseinate materials. Samples were cut into a rectangular shape (30 × 12 mm) 3−5 mm thick (measured for each individual sample). The length of the to-be-extended part was 15.2 mm. At least three measurements were performed on a fibrous protein sample in each direction, parallel and perpendicular to the shear flow (based on the shear flow−vorticity plane; thus the resulting fracture planes were the same planes as viewed by SEM). The fibrous structure led inevitably to variations between measurements because fracture sometimes occurred at once, and sometimes in multiple stages. Based on the measured force−distance curves, the Hencky strain (ϵ), tensile yield stress (σ), and Young's modulus (E) were calculated.[32]

Protein Content. The protein content of the processed samples was determined by the Dumas method using a NA2100 nitrogen and protein analyzer (CE Instruments, Milan, Italy). The nitrogen−protein conversion factor was 6.38.[33] The average measured protein content was 28.4 ± 1.1% within a 95% confidence interval. The mixed and cross-linked Ca-caseinate sample had a higher protein content of 35.4%, which was attributed to syneresis.

Results and Discussion

Macrostructural Aspects. Cross-linking with Tgase during shearing led to real fibrous macrostructures that could be torn apart along the direction of shear flow as shown in Figure 2A. The structures obtained were white and shiny. Individual macroscopic fibers, typically about 1 mm, could be observed after dispersing a piece of sample for 1 day in demineralized water (Figure 2B). Shearing of 30% Ca-caseinate without Tgase resulted in a remarkably layered structure with a subtle anisotropic character. After only the protein matrix was sheared, the opaque white structure could be peeled off in the direction of the shear flow over length scales in the order of centimeters. Ca-caseinate that was cross-linked under quiescent conditions resulted in a firm protein gel without any observable alignment. Finally, mixing of Ca-caseinate and Tgase for 35 min led to syneresis and resulted in a compact protein gel. After syneresis, the protein content of the remaining sample was 35% instead of the added 30%. Based on the macrostructural observations, it could be concluded that shear and cross-linking with Tgase appeared to be essential for creating an anisotropic fibrous Ca-caseinate structure.

Microstructure: Effect of Shear and Cross-linking. The micro- and nanoscale structures of the processed Ca-caseinate materials were studied with SEM. The SEM images of sheared and cross-linked Ca-caseinate are shown in Figure 3. Shear-induced alignment is visible in the microstructures parallel to the shear flow (Figure 3A). To give a good impression, we displayed several SEM images obtained at different magnifications and locations within the sample (Figure 3A.1, 3A.2, and 3A.3). Because of the compact microstructure, the alignment could not be observed throughout the sample. The sheared and cross-linked protein structures also contained open spaces and air bubbles, which enabled us to view fibers with a clear orientation. Those disturbances probably explain why the fiber orientation deviated from the shear direction in some cases. Figure 3A.3 shows an example of fibers at the surface of an air bubble. Obviously, the fibers viewed with SEM were on a totally different scale from the fibers observed visually in the macrostructure, that is, nanometers versus millimeters, which indicates a hierarchical fibrous structure. Based on the images, a typical fiber diameter of ∼100−200 nm could be deduced.

Perpendicular to the shear flow, two types of microstructures were observed, spherical domains of dense protein (Figure 3B.2), which may represent the cross-sections of fibers, and again aligned protein structures (Figure 3B.1 and 3B.2). The latter alignment might be caused by chained protein particles, or by an optically deceiving projection of the observed velocity gradient−vorticity plane.

The microstructure of sheared calcium caseinate without use of Tgase showed large differences as compared to the sheared and simultaneously cross-linked protein microstructures. On a macroscale, no fibers were visible, but a layered structure was formed that could be peeled off. At a microscale, a subtle orientation could be deduced from the plane parallel to the shear flow (Figure 4A.1), which was less clear for the plane perpendicular to the shear flow (Figure 4B.1). The protein network appeared more porous as compared to the cross-linked protein network (Figure 4A.2 and 4B.2), which may suggest that free water was located in those pores. The size of the protein domains was comparable to the size of the spheres that were present in the cross-linked protein network (∼100−200 nm).

Figure 5 shows the SEM images of cross-linked Ca-caseinate under quiescent conditions. The microstructures of the fracture planes parallel to the shear cell surface (Figure 5A) and perpendicular to it (Figure 5B) resembled each other. Subtle differences between these two planes could be caused by natural inhomogeneities in the material. One can observe compact areas (∼0.5 μm) surrounded by less compact areas containing protein domains. Tgase may have been present in these compact areas, and cross-linking could have led to such compactness accompanied by expulsion of free water, leading to slightly swollen and porous protein structures between the compact areas.

Finally, mixed and cross-linked Ca-caseinate yielded a compact microstructure consisting of protein spheres of ∼100 nm (Figure 6). The compactness can be explained by the

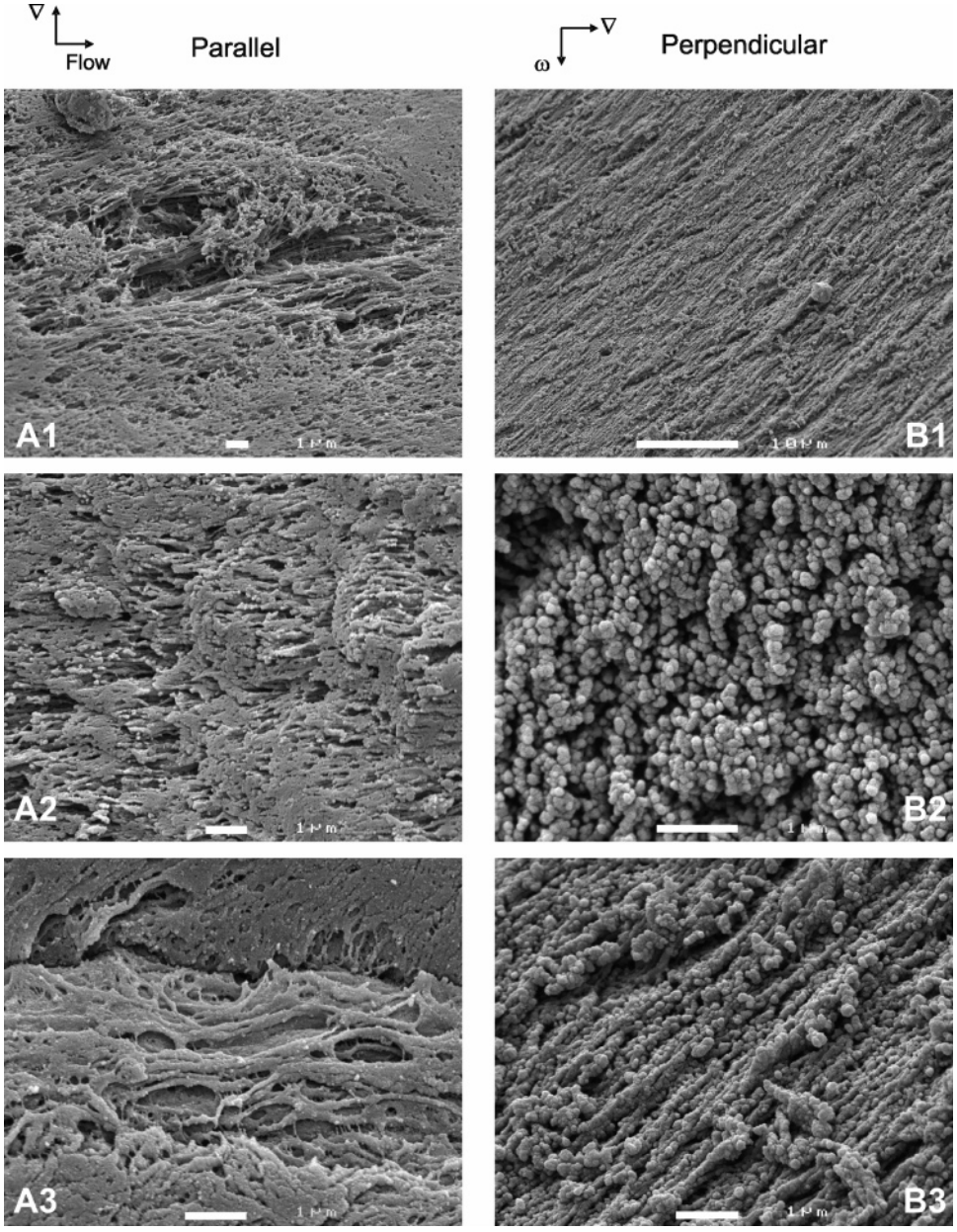

Figure 3. SEM images of fractured surfaces parallel (A) and perpendicular (B) to the shear flow exerted in the shear cell device of 30% Ca-caseinate and Tgase (E:P = 1:20) sheared at 50 °C and 50 rpm (=120 s^{-1}) during 35 min. The scale bars denote 1 μm. The images were acquired at the following magnifications: A1 at 5000×, A2 at 10 000×, A3 and B3 at 15 000×, B1 at 2500×, and B2 at 20 000×.

syneresis that occurred during mixing. No differences were observed between the randomly chosen plane 1 (Figure 6A) and the corresponding plane perpendicular to plane 1, that is, plane 2 (Figure 6B).

Summarizing, in the presence of Tgase, simple shear induced strong anisotropy on a macroscale. Alignment on a microscale was also observed, but it was not always consistent with the direction of shear flow. Only the combined action of shear and Tgase yielded anisotropic Ca-caseinate structures.

Material Properties. The material properties of the sheared and cross-linked Ca-caseinate structures are discussed in terms of their rheological and mechanical properties. The latter will reveal the anisotropic properties of the processed protein materials.

Rheological Properties. Figure 7 displays G' and tan δ within the LVE region of the various Ca-caseinate samples. Typically, the rheological properties of caseinate gels are determined by noncovalent interactions, such as electrostatic and hydrophobic interactions. The formation of covalent bonds will dominate the interactions present and will largely determine the rheological properties. Therefore, enzymatic cross-linking increased G', whereas tan δ was decreased, which is typical of structures where covalent bonds are introduced.[25,34] No difference in G' and tan δ between shearing and quiescent treatment of cross-linked Ca-caseinate was found. Thus, shearing did not affect the formation of covalent bonds. The mixed and cross-linked Ca-caseinate sample showed a larger G' and slightly lower tan δ value, which can be explained by an effective higher protein concentration.

The anisotropic behavior of the sheared and cross-linked Ca-caseinate samples was not found in the LVE properties. Only the presence of Tgase resulted in distinct differences in G' and tan δ. Therefore, we can conclude that the anisotropic fibers acted as an isotropic continuum at the length scale probed with small deformations.

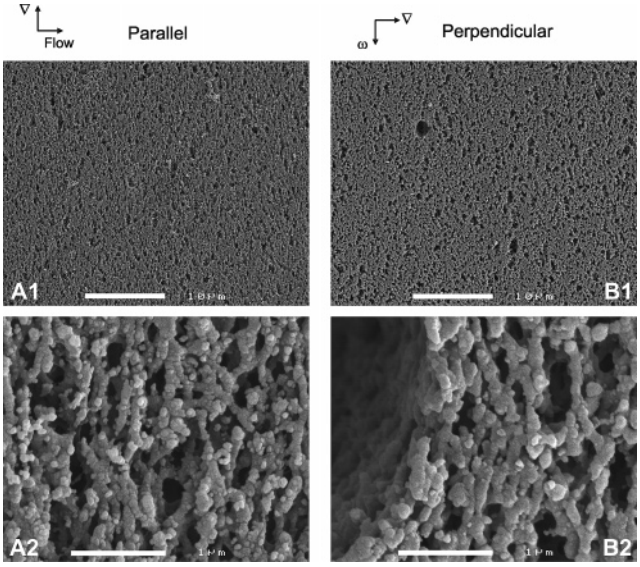

Figure 4. SEM images of fractured surfaces parallel (A) and perpendicular (B) to the shear flow exerted in the shear cell device of 30% Ca-caseinate sheared at 50 °C and 50 rpm (=120 s^{-1}) during 35 min. The scale bars denote 10 μm (A1 and B1 acquired at 3000×) and 1 μm (A2 and B2 acquired at 35 000×).

Mechanical Properties. Figure 8 depicts typical stress−strain curves of the tensile behavior of sheared and cross-linked Ca-caseinate in the two directions relative to the applied shear flow on the sample during processing. It is immediately clear that both the yield (maximum) stress and the yield strain in the parallel direction, thus in the direction of the fibers, were much larger as compared to the values in the perpendicular direction. Further, the curvature of the stress−strain curve for the sample elongated in the parallel direction showed strain hardening behavior;[10] this was not the case for the sample elongated in the other direction.

Figure 9 illustrates the tensile properties (yield stress σ, yield strain ϵ, and Young's modulus E) for the various Ca-caseinate samples that were extended until fracture. On the basis of these tensile properties, we can conclude that Ca-caseinate that was both cross-linked and sheared showed a significant degree of anisotropy because of the large differences between the properties measured in the direction parallel and perpendicular to the shear flow. Sheared Ca-caseinate behaved anisotropically, which is evident by differences in σ and ϵ (the difference in E was not significant). Cross-linked Ca-caseinate under quiescent conditions was not anisotropic based on the tensile tests; this was also observed visually and by SEM (Figure 5). When comparing the sheared Ca-caseinate sample with the sample that was cross-linked while shearing, we think that no significant amount of cross-links was formed in the direction perpendicular to the shear flow. However, these average perpendicular values of σ, ϵ, and E (Figure 9) also coincide with the perpendicular values of the quiescently cross-linked Ca-caseinate material. Apparently, the absence of mixing during the quiescently cross-linked Ca-caseinate resulted in a lack of coherence in the material. Mixed and cross-linked Ca-caseinate showed no differences in the measured stress−strain curves of the samples elongated in the two random directions perpendicular to each other. The average values of σ, ϵ, and E indicate that the material was highly elastic (high E value) and ductile (high σ value).

Table 1 summarizes the ratios between the tensile properties measured in the direction parallel and perpendicular to the shear flow. As already shown, the anisotropic fibrous samples were much stronger in the parallel direction as compared to the perpendicular direction, which was especially reflected in the high yield stress ratio $\sigma_{\parallel}/\sigma_{\perp}$ (i.e., ∼9). The ratios of the yield strain and Young's modulus were ∼2−3 for the anisotropic Ca-caseinate structures. Based on the values of the ratios of the tensile properties, the sheared Ca-caseinate in the absence of Tgase showed slight anisotropy.

Table 2 lists the values of the tensile properties, normalized with the corresponding values of the Ca-caseinate samples so that the effect of shear (sheared and cross-linked Ca-caseinate normalized with cross-linked Ca-caseinate under quiescent conditions) and of Tgase (sheared and cross-linked Ca-caseinate normalized with sheared Ca-caseinate without Tgase) could be deduced. Both shear and Tgase affected the tensile properties in the parallel direction to a large extent, that is, in the direction of the anisotropic microstructures. Moreover, considering the normalized yield stress values, the reinforcing effect of shear (in the presence of Tgase) was almost twice as large as the effect of Tgase only. This may be explained by a synergistic effect of shear and Tgase. Unfortunately, we could not determine the effect of shear in non-cross-linked Ca-caseinate, as the mechanical properties of Ca-caseinate without shearing and cross-linking could not be measured due to the weak structure. The effects of both shear and Tgase were negligible for the normalized tensile properties in the perpendicular direction, because the normalized values were close to 1.

Table 3 provides an overview of the most important macro-, microstructural, and mechanical features of the Ca-caseinate structures discussed, indicating that both shear and enzymatic cross-linking were essential for the formation of fibrous Ca-caseinate materials.

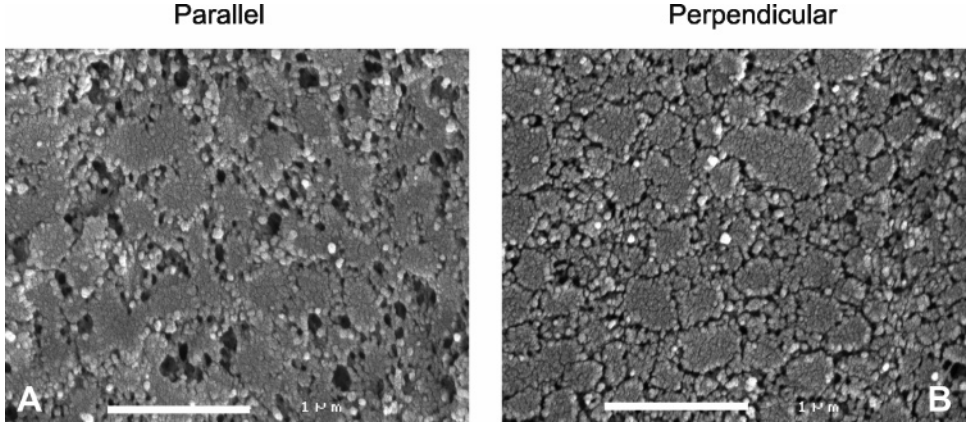

Figure 5. SEM images of parallel (A) and perpendicular (B) fractured surfaces of 30% Ca-caseinate, cross-linked by Tgase (E:P = 1:20) under quiescent conditions at 50 °C. Both images were acquired at 35 000×, and the scale bars denote 1 μm.

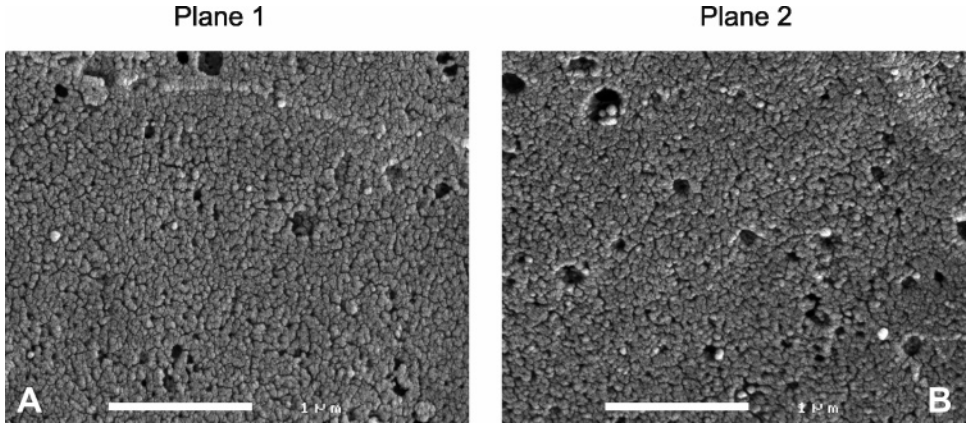

Figure 6. SEM images of fractured surfaces of 30% Ca-caseinate and Tgase (E:P = 1:20) mixed in a mixer at 50 °C and 50 rpm for 35 min. Plane 1 (A) was randomly chosen, and plane 2 (B) was perpendicular to plane 1. Both images were acquired at 35 000×, and the scale bars denote 1 μm.

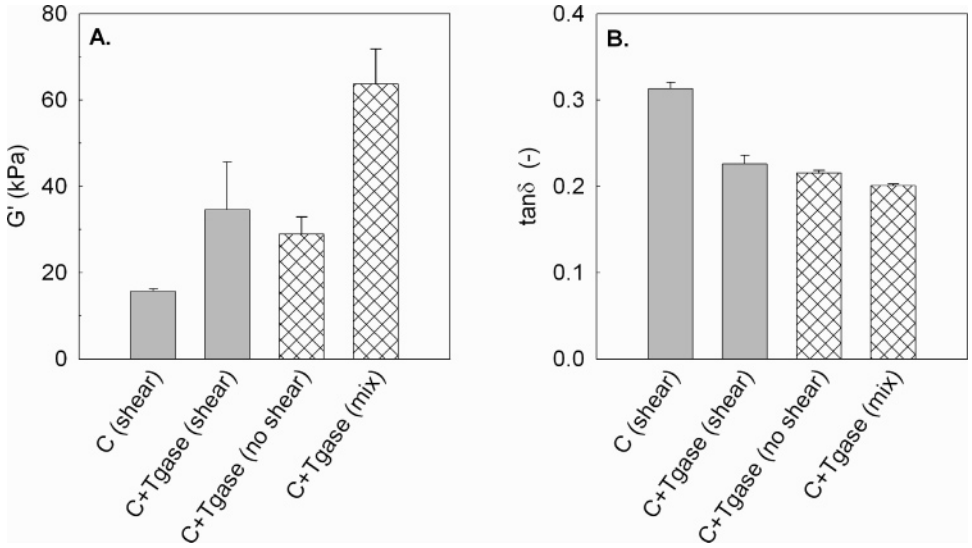

Figure 7. LVE properties *G′* (A) and tan δ (B) with 95% confidence intervals of the various 30% Ca-caseinate structures. C, Ca-caseinate; Tgase, cross-linked using Tgase; (no) shear, (un)sheared in the shear cell device; mix, mixed in mixer.

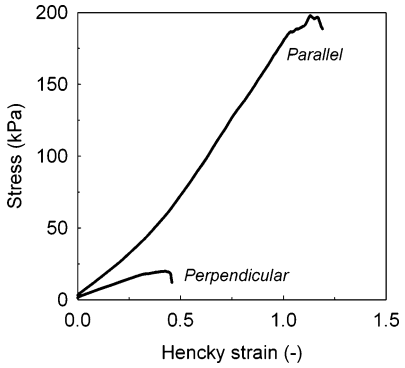

Figure 8. Typical stress−strain curves of 30% Ca-caseinate and Tgase (E:P = 1:20) sheared at 50 °C and 50 rpm (=120 s^{-1}) for 35 min, elongated in the parallel and perpendicular directions to the shear flow.

Structure Formation by Shear and Cross-linking. When a concentrated Ca-caseinate dispersion was sheared, a layered structure was found (Figure 10). Enzymatic cross-linking during shearing changed the morphology of Ca-caseinate into fibers. On the basis of the observed phenomena, we consider some factors that may account for the shear- and enzyme-induced effects.

Ca-caseinate forms aggregates of ∼100−300 nm that are stabilized due to strong interactions with Ca^{2+}-ions.[24] We assume that these structural elements are susceptible to ordering but not to breaking up. Therefore, we consider the Péclet number, which gives the ratio between convective and Brownian motion:[35]

$$Pe = \frac{6\pi a^3 \dot{\gamma} \eta_m}{kT} \quad (1)$$

where a denotes the particle radius, $\dot{\gamma}$ is the shear rate (120 s^{-1}), η_m is the viscosity of the protein medium (∼40 Pa s at the relevant shear rate, based on a measured flow curve, data not shown), k is Boltzmann's constant, and T is the temperature. When we assume a minimum protein sphere radius of 50 nm, *Pe* exceeds the critical value of 1, implicating that shear dominates in the system. Thus, alignment imposed by shear cannot be undone by diffusion. Inertia of the system is negligible for particles in the order of nanometers.

The anisotropic microstructures induced by shear and enzymatic cross-linking can be explained by phase separation of the structural elements in Ca-caseinate. It must be noted that we used a highly concentrated system, in which the casein aggregates are closely packed or in a jammed state.[36] Nevertheless, we think that local phase separation into a protein-rich and protein-poor phase with a low interfacial tension, which might have already been present in the system at rest, was enhanced by shearing, resulting in alignment of these phases.

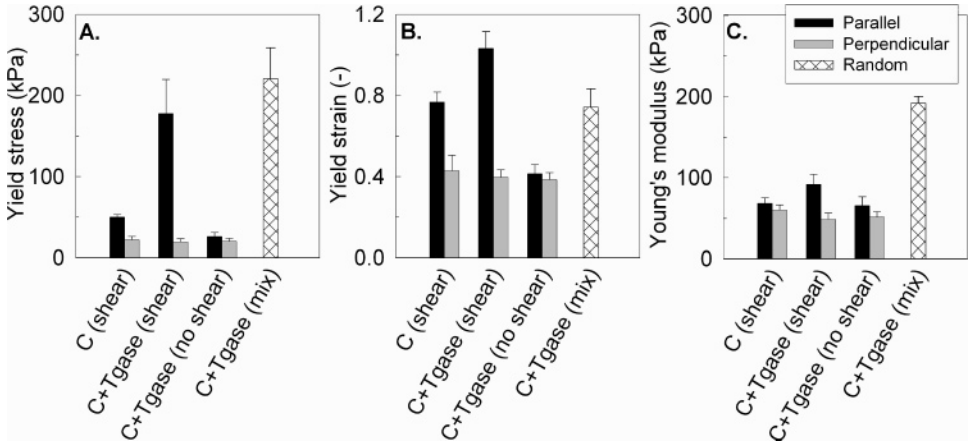

Figure 9. Tensile properties (yield stress σ, yield strain ϵ, and Young's modulus E) with 95% confidence intervals of the various 30% Ca-caseinate materials. C, Ca-caseinate; Tgase, cross-linked using Tgase (E:P = 1:20); (no) shear, (un)sheared in the shear cell device; mix, mixed in a mixer.

Table 1. Ratio of the Tensile Properties (Yield Stress σ, Yield Strain ϵ, and Young's Modulus E) Measured Parallel and Perpendicular to the Shear Flow[a]

	ratio parallel/perpendicular		
	σ	ϵ	E
C + TG − shear	9.2	2.6	1.9
C − shear	2.3	1.8	1.1

[a] The anisotropic 30% Ca-caseinate samples are sheared and cross-linked 30% Ca-caseinate (C + TG − shear) and sheared 30% Ca-caseinate (C − shear).

In the absence of Tgase, the combined effects of shear and Ca^{2+} interactions led to a layered Ca-caseinate macrostructure, which showed anisotropic behavior during the tensile tests. Vermant found that shear banding occurring in worm-likemicelle solutions yields structures that align parallel to a Couette cell wall.[37] This would result in a layered structure, similar to Figure 10A, although Vermant reported only two or three layers.[37] We suspect that, due to the close packing of the Ca-caseinate micelles, diffusion is severely hindered, which will lead to an increased number of layers. In contrast, the microstructures as observed with SEM seem to be hardly affected by shear in terms of orientation, although it is likely that alignment in Ca-caseinate at a microscale was present due to phase separation and shear. The fact that Ca-caseinate was not quenched during shearing could cause the structure to reorder due to relaxation of the aligned protein assemblies. Relaxation of dense colloidal microstructures upon cessation of shear was described for a silica−polymer system.[38]

In the presence of Tgase, cross-linking possibly increased the size of the Ca-caseinate aggregates, making them even more susceptible to alignment by shearing (*a* increases, consequently *Pe* increases). In addition, in the phase-separated protein-rich phase, Tgase induced covalent bonds in the direction of the flow. Shear-induced anisotropy in polystyrene particle suspensions was attributed to the directional dependence of break-up and reformation of aggregates.[39] Because solidification occurred at a shorter time scale than relaxation, the fibrous micro- and macrostructures were preserved after cessation of shear. On the basis of these considerations, we think that the anisotropy in the samples starts at the molecular level. Enhanced anisotropy as a result of enzymatic action eventually leads to macroscopical anisotropy.

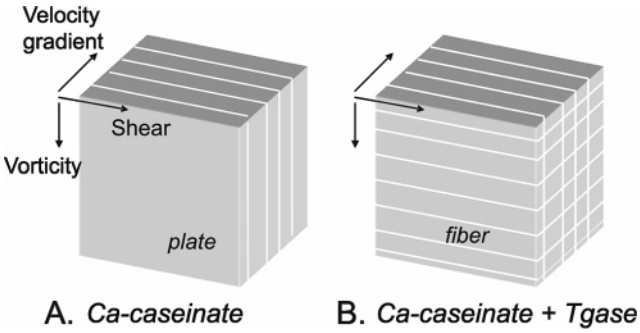

Figure 10. Schematic overview of shear- and enzyme-induced anisotropy in the dense Ca-caseinate: layered structure as observed after shearing Ca-caseinate (A) and the fibrous structure as observed after shearing Ca-caseinate in the presence of Tgase (B).

Process Prospective. In this paper, we used an in-house-developed shearing device to be able to use shear rate as a process parameter. Although the use of simple shear is well known in rheological studies, it is rare in conventional processing. Our results, however, show that it may be interesting to consider the use of simple shear in processes, as it leads to the creation of novel structures that can be used in novel food

Table 2. Normalized Tensile Properties (Yield Stress σ, Yield Strain ϵ, and Young's Modulus E) for the Measured Parallel and Perpendicular Directions[a]

		parallel, normalized			perpendicular, normalized		
		σ	ϵ	E	σ	ϵ	E
effect shear	$\frac{[C + TG]_{shear}}{[C + TG]_{noshear}}$	7.7	2.6	1.6	0.8	1.0	0.8
effect Tgase	$\frac{[C + TG]_{shear}}{[C]_{shear}}$	3.5	1.3	1.4	0.9	0.9	0.8

[a] The sheared and cross-linked 30% Ca-caseinate sample (C + TG − shear) was normalized with cross-linked 30% Ca-caseinate under quiescent conditions (C + TG − no shear), and with the sheared 30% Ca-caseinate (C − shear), leading to the effect of shear and Tgase, respectively.

Table 3. Overview of the Macro-, Microscale, and Mechanical Characteristics of 30% Ca-Caseinate Samples after Shearing, Mixing, or Quiescent Treatment, with or without Tgase

	property	Ca-caseinate	Ca-caseinate + Tgase
shearing	macro[a]	layered	fibers <1 mm
	micro[b]	little orientation, protein domains ~60−120 nm	fibers ~100−200 nm
	mechanical[c]	slightly anisotropic	highly anisotropic
quiescent	macro[a]	isotropic, grainy[d]	isotropic
	micro[b]		protein domains ~50−100 nm and patches ~200−700 nm
	mechanical[c]		isotropic
mixing	macro[a]		isotropic
	micro[b]		protein domains ~100 nm
	mechanical[c]		isotropic

[a] Macro denotes the macrostructural properties of the Ca-caseinate materials after processing. [b] Micro denotes the microstructural characteristics as observed with SEM. [c] Mechanical denotes the behavior of the Ca-caseinate materials during tensile tests (i.e., isotropic or anisotropic). [d] Sample was not cohesive enough to perform SEM and mechanical analysis.

products. This leads to the question of whether such a shearing device can be scaled up to an industrial process.

A constant shear profile can be obtained or approached using a cone and plate configuration, but also in a Couette configuration. The latter configuration may be more appropriate for scaling up, as the outer cylinder resembles current industrial vessels. By changing the conventional stirrer, one could possibly obtain a neat shear field inside the reactor. The process that we present in this paper is carried out at constant temperature. Therefore, we do not impose any limitations concerning heating or cooling to the process, which will ease the scale up to industrial scale.

To conclude, development of new processing equipment seems essential for making the fibrous structures presented here. Fortunately, the conditions used in this study may be applicable at industrial scale.

Conclusions

We have shown that an anisotropic fibrous Ca-caseinate structure was formed using a novel technology based on shear-induced structure formation and concurrent solidification. Enzymatic cross-linking during shearing proved to be essential for the anisotropic structure formation. The simplicity of the method combined with the high anisotropy obtained show the potential of the technology for novel food structures and applications.

After shearing and enzymatic cross-linking using Tgase, anisotropic fibrous structures were formed in a concentrated Ca-caseinate matrix on the macroscale and the microscale. We visually observed fibers of about 1 mm, and the SEM images revealed protein fibers with a diameter of ~100−200 nm, which were composed of chained protein domains. The LVE properties showed an increase in G' and a decrease in tan δ due to addition of Tgase. These properties were isotropic (i.e., independent of the direction of strain). In contrast, tensile properties confirmed the presence of anisotropic structures, especially based on large differences between the yield stress values in the parallel and perpendicular directions as compared to the applied shear flow. Shear affected the reinforcement of the anisotropic fibers to a large extent, whereas the properties in the perpendicular direction remained constant. Tgase also significantly influenced the structure formation in the shear direction.

Phase separation of protein aggregates at a molecular level due to shear was proposed as the mechanism leading to shear- and enzyme-induced anisotropic structures. Enzymatic cross-linking is needed to solidify the aligned protein aggregates, which may relax on cessation of shear when no solidification agent is present. Therefore, we conclude that macroscopic alignment is due to phenomena at a molecular scale.

Acknowledgment. This project was supported by a grant from the Dutch Programme EET (Economy, Ecology, Technology), a joint initiative of the Ministries of Economic Affairs, Education, Culture and Sciences and of Housing, Spatial Planning and the Environment. The programme is managed by the EET Programme Office, SenterNovem. We are grateful to A. van Aelst from the Wageningen Electron Microscopy Centre for preparing the SEM images. M. Paques, F. J. H. Jeurissen, and J. de Slegte from Friesland Foods are thanked for valuable discussions.

References and Notes

(1) Aguilera, J. M. *J. Food Eng.* **2005**, *67*, 3−11.
(2) Aguilera, J. M.; Stanley, D. W. *Food Rev. Int.* **1993**, *9*, 527−550.
(3) Akkermans, C.; Venema, P.; Rogers, S. S.; Van der Goot, A. J.; Boom, R. M.; Van der Linden, E. *Food Biophys.* **2006**, *1*, 144−150.
(4) Veerman, C.; Sagis, L. M. C.; Venema, P.; van der Linden, E. *J. Rheol.* **2005**, *49*, 355−368.
(5) Cheftel, J. C.; Kitagawa, M.; Queguiner, C. *Food Rev. Int.* **1992**, *8*, 235−275.
(6) Noguchi, A. Extrusion cooking of high-moisture protein foods. In *Extrusion Cooking*; Mercier, C., Linko, P., Harper, J. M., Eds.; American Association of Cereal Chemists, Inc.: St. Paul, MN, 1989; pp 343−370.
(7) Thiebaud, M.; Dumay, E.; Cheftel, J. C. *Lebensm.-Wiss. Technol.-Food Sci. Technol.* **1996**, *29*, 526−535.
(8) Liu, S. X.; Peng, M.; Tu, S.; Li, H.; Cai, L.; Yu, X. *Food Sci. Technol. Int.* **2005**, *11*, 463−470.
(9) Tolstoguzov, V. B. *J. Am. Oil Chem. Soc.* **1993**, *70*, 417−424.
(10) Peighambardoust, S. H.; Van der Goot, A. J.; Van Vliet, T.; Hamer, R. J.; Boom, R. M. *J. Cereal Sci.* **2006**, *43*, 183−197.
(11) Van den Einde, R.; Van der Linden, E.; Van der Goot, A. J.; Boom, R. *Polym. Degrad. Stab.* **2004**, *85*, 589−594.
(12) Gallant, D. J.; Bouchet, B.; Culioli, J. *Food Microstruct.* **1984**, *3*, 175−183.
(13) Downey, G.; Burgess, K. J. *J. Food Technol.* **1979**, *14*, 21−31.
(14) Downey, G.; Burgess, K. J. *J. Food Technol.* **1979**, *14*, 33−40.
(15) Antonov, Y. A.; Zhuravskaya, N. A.; Tolstoguzov, V. B. *Nahrung* **1985**, *29*, 39.
(16) Suchkov, V. V.; Grinberg, V. J.; Tolstoguzov, V. B. *Nahrung-Food* **1980**, *24*, 893−897.
(17) Suchkov, V. V.; Grinberg, V. Y.; Bikbov, T. M.; Muschiolik, G.; Schmandke, H.; Tolstoguzov, V. B. *Nahrung-Food* **1988**, *32*, 669−678.
(18) Suchkov, V. V.; Popello, I. A.; Bikbov, T. M.; Grinberg, V. Y.; Dianova, V. T.; Polyakov, V. I.; Muschiolik, G.; Schubring, R.; Schmandke, H.; Tolstoguzov, V. B. *Nahrung-Food* **1988**, *32*, 679−689.

(19) Rampon, V.; Robert, R.; Nicolas, N.; Dufour, E. *J. Food Sci.* **1999**, *64*, 313−316.
(20) De Kruif, C. G. Caseins. In *Industrial Proteins in Perspective*; Aalbersberg, W. Y., Hamer, R. J., Jasperse, P., de Jongh, H. H. J., De Kruif, C. G., Walstra, P., de Wolf, F. A., Eds.; Elsevier Science: Amsterdam, 2003; Vol. 23, pp 219−262.
(21) Moughal, K. I.; Munro, P. A.; Singh, H. *Int. Dairy J.* **2000**, *10*, 683−690.
(22) Srinivasan, M.; Singh, H.; Munro, P. A. *Int. Dairy J.* **1999**, *9*, 337−341.
(23) De Kruif, C. G. *J. Dairy Sci.* **1998**, *81*, 3019−3028.
(24) Dickinson, E.; Semenova, M. G.; Belyakova, L. E.; Antipova, A. S.; Il'in, M. M.; Tsapkina, E. N.; Ritzoulis, C. *J. Colloid Interface Sci.* **2001**, *239*, 87−97.
(25) Manski, J. M.; Van der Goot, A. J.; Boom, R. M. *J. Food Eng.* **2007**, *79*, 706−717.
(26) Lorenzen, P. C.; Schlimme, E.; Roos, N. *Nahrung-Food* **1998**, *42*, 151−154.
(27) Nonaka, M.; Sakamoto, H.; Toiguchi, S.; Kawajiri, H.; Soeda, T.; Motoki, M. *J. Food Sci.* **1992**, *57*, 1214−1218.
(28) Lucey, J. A.; Srinivasan, M.; Singh, H.; Munro, P. A. *J. Agric. Food Chem.* **2000**, *48*, 1610−1616.
(29) Yokoyama, K.; Ohtsuka, T.; Kuraishi, C.; Ono, K.; Kita, Y.; Arakawa, T.; Ejima, D. *J. Food Sci.* **2003**, *68*, 48−51.
(30) Peighambardoust, S. H.; Van der Goot, A. J.; Hamer, R. J.; Boom, R. M. *Cereal Chem.* **2004**, *81*, 714−721.
(31) Muller, W. H.; van Aelst, A. C.; Humbel, B. M.; van der Krift, T. P.; Boekhout, T. *Scanning* **2000**, *22*, 295−303.
(32) Gunasekaran, S.; Ak, M. M. Fundamental rheological methods. *Cheese Rheology and Texture*; CRC Press: Boca Raton, FL, 2003; pp 31−112.
(33) Guo, M. R.; Fox, P. F.; Flynn, A.; Kindstedt, P. S. *Int. Dairy J.* **1996**, *6*, 473−483.
(34) Dickinson, E.; Yamamoto, Y. *J. Agric. Food Chem.* **1996**, *44*, 1371−1377.
(35) Larson, R. G. *The Structure and Rheology of Complex Fluids*; Oxford University Press: New York, 1999; pp 263−323.
(36) Panouille, M.; Durand, D.; Nicolai, T. *Biomacromolecules* **2005**, *6*, 3107−3111.
(37) Vermant, J. *Curr. Opin. Colloid Interface Sci.* **2001**, *6*, 489−495.
(38) Ramakrishnan, S.; Gopalakrishnan, V.; Zukoski, C. F. *Langmuir* **2005**, *21*, 9917−9925.
(39) Hoekstra, H.; Vermant, J.; Mewis, J. *Langmuir* **2003**, *19*, 9134−9141.

BM061008P